

Flexible PVC flame retarded with expandable graphite

Walter Wilhelm Focke^{1,*}, Herminio Muiambo¹, Washington Mhike¹, Hermanus Joachim Kruger¹ and Osei Ofosu²

¹SARChI Chair in Carbon Technology and Materials, Institute of Applied Materials, Department of Chemical Engineering, University of Pretoria, Private Bag X20, Hatfield 0028, South Africa

²CSIR Materials Science and Manufacturing, PO Box 1124, Port Elizabeth 6000, South Africa

Abstract

The utility of expandable graphite as a flame retardant for PVC, plasticized with 60 phr of a phosphate ester, was investigated. Cone calorimeter results, at a radiant flux of 35 kW m^{-2} , revealed that adding only 5 wt.% expandable graphite lowered the peak heat release rate from $325 \pm 11 \text{ kW m}^{-2}$ to $63 \pm 23 \text{ kW m}^{-2}$ and the total heat release from $55 \pm 11 \text{ MJ m}^{-2}$ to only $10.7 \pm 0.3 \text{ MJ m}^{-2}$. All samples containing expandable graphite ignited and burned only very briefly before flame out. The remarkable effectiveness of the expandable graphite is attributed to an excellent match between the exfoliation onset temperature of the graphite and the onset of decomposition of the PVC. This means that the exfoliation of the graphite forms a protective barrier layer at the right place at the right time. In addition, the simultaneous release of halogen species by the polymer matrix and the exfoliating graphite prevents the formation of a flammable air fuel mixture.

Keywords: Expandable graphite; graphite oxide; graphite intercalation compound; exfoliation; thermal analysis

*Corresponding author: Tel: +27 12 420 3728. Fax: +27 12 420 2516. E-mail address: walter.focke@up.ac.za (W.W. Focke)

1. Introduction

PVC is a very versatile polymer used in diverse applications including flooring, rigid pipes, flexible hoses, conveyor belting, wire- and cable-insulation. Neat PVC features a relatively high chlorine content of 56.7 wt.%. That makes it more resistant to ignition and burning than

most organic polymers [1]. However, the conventional plasticisers used in the manufacture of flexible PVC detract from this outstanding fire resistance. Thus flame-retardant (FR) and smoke-suppressant (SS) additives must be incorporated in order to meet product test specifications such as oxygen index, heat release rate, smoke evolution, or the extent of burning [1]. Levchik and Weil [2] and Weil *et al.* [3] reviewed the chemical additives that have been considered to achieve acceptable fire properties in the principal PVC application areas. In particular, phosphate esters are useful as flame retardant plasticizers in flexible PVC [2].

Neat PVC is thermally unstable and prone to autocatalytic dehydrochlorination [4]. Addition of thermal stabilizers are required to allow processing at elevated temperatures [5]. However, pyrolysis of PVC yields a isotropic carbon char residue [6] and this contributes to the mechanisms of flame retardant action [5].

Expandable graphite (EG) is a partially oxidized form of graphite containing intercalated guest species (e.g., sulfuric acid anions) in-between the stacked graphene layers [7, 8]. Commercially expandable graphite is made via liquid-phase graphite – sulfuric acid reactions in the presence of strong chemical oxidants such as KMnO_4 , HNO_3 and H_2O_2 [7, 9, 10]. A key property of expandable graphite is its tendency to exfoliate when heated to high temperatures. During exfoliation it expands rapidly in a worm-like manner to form vermicular graphite with a low density [11-13]. The exfoliation process is an endothermic event and the expansion shows ideal gas law behaviour. According to Chung [12], the origin of this process lies in the vaporization of the intercalate. This implies that the gases that cause the explosive expansion of the expandable graphite mainly comprise CO_2 and SO_2 [8].

Expandable graphite (EG) is a good intumescent flame retardant for many polymers [14-17] and in particular for polyethylene [18] and polyurethane foam [8, 17]. Expandable graphite has similar in-plane electrical conductivity as natural flake graphite [19]. This means that it

could impart both antistatic and flame retardant properties to polymers [20]. However, the use of expandable graphite as a flame retardant additive in PVC has not yet been reported. The objective of this study was to make a small contribution in this regard.

2. Materials and methods

2.1. Materials

Expandable graphite grade ES 250 B5 was obtained from Qingdao Kropfmuehl Graphite (China). Exfoliated graphite form was prepared at a temperature of 600 °C by placing the expandable graphite powder samples in a Thermopower electric furnace. Milled natural Zimbabwean flake graphite (Graphite) was supplied by BEP Bestobell (South Africa) and used as a reference material. TPC Paste Resin Co., Ltd. supplied the poly(vinyl chloride) emulsion grade PG680. It was a free flowing powder with a K-value of 69. Reofos 50, a synthetic isopropylated triaryl phosphate ester plasticizer, was supplied by Chemtura.

2.2. Preparation of the graphite-PVC composites

The 20 wt.% graphite compound was prepared using the plastisol route. PVC powder (100 g), Reofos 50 (60 g) and expandable graphite (40g) were mixed together in a high shear mixer for 15 minutes. The paste mixture was immediately poured into a mould (100 mm × 100 mm × 4 mm) and heated for 10 minutes in a convection oven set at 130 °C. Thereafter the sheets were cured at 150 °C and 10 MPa in a hot press for 5 minutes. Other samples were made in a similar way by varying the expandable graphite content but keeping the plasticizer level fixed at 60 parts per 100 parts PVC resin.

2.3. Particle size, BET surface and density determination

The graphite particle size distributions were determined with a Mastersizer Hydrosizer 2000MY (Malvern Instruments, Malvern, UK). The specific surface areas of the graphite powders were determined on a Micromeritics Flowsorb II 2300 and a Nova 1000e BET instrument in N₂ at 77 K. Densities were determined on a Micromeritics AccuPyc II 1340 helium gas pycnometer.

2.4. Scanning Electron Microscopy (SEM)

Graphite morphologies were studied using a JEOL JSM 5800LV scanning electron microscope (SEM). The acceleration voltages used in this instrument was 20 kV. No electro-conductive coating was applied on the graphite particles.

2.5. Thermogravimetry (TGA)

Thermogravimetric analysis (TGA) was performed using the dynamic method on a Mettler Toledo A851 TGA/SDTA instrument. About 5 mg sample was placed in an open 150 μ L alumina pan. Temperature was scanned from 25 °C to 900 °C at a scan rate of 10 °C min⁻¹ with air flowing at a rate of 50 mL min⁻¹.

2.6. Graphite composition determinations

The composition of the graphite powder was determined by XRF analysis performed using a wavelength-dispersive spectrometer (ARL 9400XP+ XRF). The samples were prepared as pressed powder briquettes and introduced to the spectrometer. The powder was ground in a tungsten carbide milling vessel and roasted at 1000°C for determination of the loss on ignition (LOI).

2.7. Thermomechanical analysis

Thermal expansion measurements were conducted on a TA instruments Q400 Thermo Mechanical Analyzer. Sufficient expandable graphite powder was placed in an alumina sample pan such that the bed height was between 35 μm and 40 μm . The flake expansion behaviour was measured with a flat-tipped standard expansion probe using an applied force of 0.02 N. The temperature was scanned from 30 $^{\circ}\text{C}$ to 1000 $^{\circ}\text{C}$ at a scan rate of 10 $^{\circ}\text{C min}^{-1}$ in nitrogen atmosphere. The expansion relative to the original powder bed height was reported.

2.8. Cone calorimeter test

The ISO 5660-1 standard was followed in performing the cone calorimeter tests using a Dual Cone Calorimeter (Fire Testing Technology (UK) Ltd.). Three specimens of each composition were tested. The sheet dimensions were 100 mm \times 100 mm \times 4 mm. They were placed on aluminium foil and exposed horizontally to an external heat flux of 35 kW m^{-2} .

3. Results and Discussion

3.1. Graphite particle characterization

The d_{10} , d_{50} , and d_{90} particle sizes, BET surface area, and densities of the graphite samples are presented in Table 1. The surface area of the neat ES250 B5 could not be determined as it started to exfoliate during the BET measurements. Figure 1 shows the flake-like nature of the natural and expandable graphite. The exfoliated graphite samples in Figure 1 have worm-shaped, accordion-like structures. Slit-shaped gaps between the graphite platelets are clearly visible in the high resolution micrographs.

The accordion-like microstructure of the expanded worms is built up of distorted graphite sheets. The average thickness of these sheets can be estimated from the BET surface area using the equation

$$t = 2/\rho A \quad (1)$$

Where t is the average sheet thickness in m, ρ is the density in kg m^{-3} ; and A is the BET surface area in $\text{m}^2 \text{kg}^{-1}$. Note that equation (1) neglects the edge surface area of the flakes.

Applying this equation to the expanded graphite sample yielded an average flake thickness of about 40 nm. This confirms the nanostructured nature of the expanded “worms”.

XRF results shown in Table 2 reveal that the inorganic content of the Zimbabwean flake graphite was about 8 wt.%. The main impurities appeared to be silica and clay minerals. According to the XRF results, the apparent carbon content of the expandable graphite sample was about 88 wt.%. The XRF results provide a hint on how the expandable graphite sample was made. Compared to the natural graphite, the ES250 grade contains manganese and potassium suggesting that KMnO_4 was used as oxidant in its manufacture.

3.2. Thermogravimetry (TGA) and thermomechanical analysis (TMA)

Figure 2 shows the TGA mass loss curves for the neat plasticized PVC, expandable graphite and a compound containing 20 wt.% EG. The exfoliation of the expandable graphite grade occurs in two steps. The onset temperature in the TGA is about 190 °C and the DTG peaks (not shown) occur at 223 °C and 409 °C. By 600 °C the EG sample has lost 17 wt.%. At higher temperatures all samples oxidize and rapidly lose mass. However, the natural graphite shows significantly higher oxidative stability. The key result from Figure 2 is the near perfect match between the exfoliation onset temperature of the expandable graphite and the decomposition onset temperature of the PVC compound. The present PVC expandable graphite system thus conforms to the “in the right place at the right time” flame retardant

principle. It is also clear that the presence of the expandable graphite, unlike many other fire retardant additives, did not lower the degradation temperature of the matrix polymer.

A key property of expandable graphite is the ability to exfoliate in narrow temperature range.

Figure 3 shows the expansion behaviour of the graphite samples as characterized by TMA.

The TMA exfoliation onset temperature for the EG was about 225 °C.

3.3. Flammability

The cone calorimeter results are presented in Figure 4 to Figure 11 and they are summarized in Table 3. Figure 4 shows representative heat release rate (HRR) curves obtained from the cone calorimeter tests. All the neat PVC compound samples ignited and flamed briefly. This gave rise to the sharp peak in the HRR at short times. One of the PVC samples subsequently re-ignited and burned. It is the HRR curve for this sample that is plotted in Figure 4. All the neat PVC samples produced a large amount of smoke. The heat release curves for the neat plasticized PVC compound exhibited the shape characteristic of thermally thin samples [21]. Thermally thin samples are identified by a sharp peak in their HRR curves as the whole sample is pyrolyzed at once.

HRR curves characteristic of thermally thick, char-producing samples show a sudden rise to a plateau value [21]. However, the HRR curves for the samples containing expandable graphite were more complex. They showed a sharp peak at short times and a second flatter and broader curve at longer times. The PVC-EG composites ignited and flamed briefly during the time period corresponding to the first peak in the HRR. However, compared to the neat PVC compound, the first sharp peak in the HRR for the PVC-EG composites was much reduced in intensity. Neither a second ignition nor a visible flame was observed during the time period corresponding to the second HRR peak. However, profuse smoke evolution continued. This suggests the PVC-EG composites samples were pyrolyzed while at the same time a glowing

combustion occurred at the surface during the second part of the test. All the EG-containing samples left an expanded residue.

Figure 5 shows the effect of adding EG to PVC on the peak heat release rates (pHRR) and the total heat release. The pHRR results are also tabulated in Table 3. The pHRR for the neat PVC compound was $325 \pm 11 \text{ kW m}^{-2}$. The best result was obtained with 20 wt.% EG ($20 \pm 8 \text{ kW m}^{-2}$) but even with 5 wt.% EG the value was $63 \pm 23 \text{ kW m}^{-2}$. Adding expandable graphite, even at the 5 wt.% level, caused a significant lowering of the pHRR. Similar observations hold for the total heat release. It was $55 \pm 11 \text{ MJ m}^{-2}$ for the neat PVC compound and only $10.7 \pm 0.3 \text{ MJ m}^{-2}$ for the compound with 5 wt.% EG. Adding 20 wt.% EG decreased the total heat release value to only $2.2 \pm 1.1 \text{ MJ m}^{-2}$. The improved fire performance with respect to the peak heat release rate and the total heat release is attributed to a combination of factors. Firstly the expansion of the EG formed a low density layer of ‘worm like’ structures that provided a protective barrier at the polymer surface. This limited heat transfer to the substrate and thus slowed down the rate of thermal degradation. Figure 6 confirms that the addition of the EG reduced the mass loss rate (MLR). Secondly, the gases concurrently released by the exfoliation of the EG (CO_2 and SO_2) and the release of the HCl by the decomposing PVC apparently also prevented flaming combustion during the latter part of the cone calorimeter tests. This can be attributed to a dilution effect on the air-fuel mixture in the gas phase. However, the halogen entering the gas phase also contributed to a “flame poisoning effect”, i.e. the slowing down of the free radical chain reactions occurring in the flame [3]. In combination, these two effects explain why the cone calorimeter test proceeded without a visible flame following an initial short-lived ignition. It degenerated into a bulk pyrolysis experiment in combination with a surface glowing-combustion event.

Figure 7 plots the times to ignition and time to flame out for the various samples. The time to ignition (t_{ig}) was $35 \pm 3 \text{ s}$ for the neat PVC compound and $28 \pm 3 \text{ s}$ for the compound

containing 5 wt.% EG but increased to 40 ± 9 for the compound containing 20 wt.% EG. See Table 3. Adding EG also reduced the time to flame out considerably.

Figure 8 compares the smoke production rates (SPR) of the composites with that for the neat PVC compound. The expandable graphite composites featured lower SPRs owing to the reduction in the rate of mass loss. Figure 9 and Figure 10 show the CO₂ and CO release rates. The observed trends mirror those observed for the HRR (Figure 4) almost perfectly. After 150 s the CO₂ emission rates dropped to very low values. This is, in part, a consequence of the non-flaming degradation during the latter part of the cone calorimeter tests.

The fire growth rate (FIGRA) and the maximum average rate of heat emission (MAHRE) are indices that may be used to interpret cone calorimeter data [21, 22]. The FIGRA is an estimator for the fire spread rate and size of the fire whereas the MARHE guesstimates the tendency of a fire to develop [22]. The FIGRA is determined as

$$FIGRA = pHRR/time\ to\ pHRR \quad (2)$$

Table 3 lists the FIGRA and MAHRE indices. Marked decreases of up to 50% relative to the neat PVC compound were observed for the FIGRA as the EG content was increased to 20 wt.%. At the same time the MAHRE decreased by almost a factor of six.

The parameters that are pertinent to fire hazards are the fire load and flame spread [21]. The Petrella plot is an attempt to gauge the magnitude of the fire hazard posed [21, 23]. It is a plot of the total heat released tHR (as fireload) against $pHRR/t_{ig}$ (as a fire growth index). Figure 11 shows a Petrella plot for the composites fabricated in this work. For a material to be effectively flame retarded both the fire load and the fire growth index should assume low values. Figure 11 shows a dramatic decrease for all the EG composites relative to the neat PVC compound. It shows that expandable graphite is a very effective flame retardant for the plasticized PVC considered in this study.

4. Conclusions

Emulsion grade PVC was plasticized with 60 phr of a phosphate ester. The effect of adding expandable graphite on the fire behaviour of this material was studied using the cone calorimeter. The addition of expandable graphite significantly improved the fire resistance of the plasticized PVC. Even adding only 5 wt.% expandable graphite lowered the peak heat release rate from $325 \pm 11 \text{ kW m}^{-2}$ to $63 \pm 23 \text{ kW m}^{-2}$ and the total heat release from $55 \pm 11 \text{ MJ m}^{-2}$ to only $10.7 \pm 0.3 \text{ MJ m}^{-2}$. All the samples containing expandable graphite ignited and burned very briefly before flame out. However, after the flame out, they continued to emit smoke and low concentrations of the combustion gases CO_2 and CO . This is attributed to pyrolysis and glowing combustion of the exposed surface during the latter part of the cone calorimeter tests. The Petrella plot (Figure 11), which provides a measure of the flame retarding effect in the composites encompassing the fire load (total heat evolved) and fire growth index, confirmed the expandable graphite as a very effective flame retardant for the plasticized PVC. The remarkable effectiveness of the expandable graphite is attributed to two main factors. First is the voluminous expansion of the expandable graphite at the exposed surface. It generates a thermal barrier to heat transfer to the substrate below. This slows the rate of pyrolysis and reduces the rate at which combustible fuel is produced. The second factor is the good match between the exfoliation onset temperature of the graphite and the onset of decomposition of the PVC as revealed by thermogravimetric analysis. This means that the halogen flame poison (HCl) formed by the degradation of the PVC matrix and the inert gases from the exfoliation of the expandable graphite (CO_2 and SO_2) are released simultaneously. They suppress the free radical reactions in the gas phase and dilute the flammable air fuel mixture sufficiently to cause early flame out after the initial ignition event. They also prevent a re-ignition and further pyrolysis proceeds without a visible flame

although the continued release of CO (and CO₂) indicated that glowing combustion must have continued at the outer surface directly exposed to the heat flux from the cone.

Acknowledgements

This work is based upon research supported by the South African Research Chairs Initiative of the Department of Science and Technology (DST) and the National Research Foundation (NRF). Any opinion, findings and conclusions or recommendations expressed in this material are those of the authors and therefore the NRF and DST do not accept any liability with regard thereto.

References

- [1] Coaker AW. Fire and flame retardants for PVC. *Journal of Vinyl and Additive Technology*. 2003;9:108-15.
- [2] Levchik SV, Weil ED. Overview of the recent literature on flame retardancy and smoke suppression in PVC. *Polymers for Advanced Technologies*. 2005;16:707-16.
- [3] Weil ED, Levchik S, Moy P. Flame and smoke retardants in vinyl chloride polymers - Commercial usage and current developments. *Journal of Fire Sciences*. 2006;24:211-36.
- [4] Starnes Jr WH, Ge X. Mechanism of autocatalysis in the thermal dehydrochlorination of poly(vinyl chloride). *Macromolecules*. 2004;37:352-9.
- [5] Folarin OM, Sadiku ER. Thermal stabilizers for poly(vinyl chloride): A review. *International Journal of Physical Sciences*. 2011;6:4323-30.
- [6] Otani S. On the carbon fiber from the molten pyrolysis products. *Carbon*. 1965;3:31-8.
- [7] Furdin G. Exfoliation process and elaboration of new carbonaceous materials. *Fuel*. 1998;77:479-85.
- [8] Camino G, Duquesne S, Delobel R, Eling B, Lindsay C, Roels T. Mechanism of Expandable Graphite Fire Retardant Action in Polyurethanes. *Fire and Polymers: American Chemical Society*; 2001. p. 90-109.
- [9] Sorokina NE, Shornikova ON, Avdeev VV. Stability limits of graphite intercalation compounds in the systems graphite-HNO₃(H₂SO₄)-H₂O-KMnO₄. *Inorganic Materials*. 2007;43:822-6.
- [10] Celzard A, Marêché JF, Furdin G. Modelling of exfoliated graphite. *Progress in Materials Science*. 2005;50:93-179.
- [11] Wissler M. Graphite and carbon powders for electrochemical applications. *Journal of Power Sources*. 2006;156:142-50.
- [12] Chung DDL. Exfoliation of graphite. *Journal of Materials Science*. 1987;22:4190-8.
- [13] Chung DDL. Review: Graphite. *Journal of Materials Science*. 2002;37:1475-89.
- [14] Weil ED, Levchik SV. Flame retardants in commercial use or development for polyolefins. *Journal of Fire Sciences*. 2008;26:5-43.

- [15] Weil ED. Fire-protective and flame-retardant coatings - A state-of-the-art review. *Journal of Fire Sciences*. 2011;29:259-96.
- [16] Chen L, Wang YZ. A review on flame retardant technology in China. Part I: Development of flame retardants. *Polymers for Advanced Technologies*. 2010;21:1-26.
- [17] Nakagawa Y. Recent development of flame retardant polymeric materials containing expandable graphite. *Bulletin of Japan Association for Fire Science and Engineering*. 2006;56:37-43.
- [18] Qu B, Xie R. Intumescent char structures and flame-retardant mechanism of expandable graphite-based halogen-free flame-retardant linear low density polyethylene blends. *Polymer International*. 2003;52:1415-22.
- [19] Zheng W, Lu X, Wong SC. Electrical and mechanical properties of expanded graphite-reinforced high-density polyethylene. *Journal of Applied Polymer Science*. 2004;91:2781-8.
- [20] Mhike WF, W.W. Surface resistivity and mechanical properties of rotationally molded polyethylene/graphite composites. *Journal of Vinyl and Additive Technology*. 2013.
- [21] Schartel B, Hull TR. Development of fire-retarded materials—Interpretation of cone calorimeter data. *Fire and Materials*. 2007;31:327-54.
- [22] Sacristán M, Hull TR, Stec AA, Ronda JC, Galià M, Cádiz V. Cone calorimetry studies of fire retardant soybean-oil-based copolymers containing silicon or boron: Comparison of additive and reactive approaches. *Polymer Degradation and Stability*. 2010;95:1269-74.
- [23] Petrella RV. The Assessment of Full-Scale Fire Hazards from Cone Calorimeter Data. *Journal of Fire Sciences*. 1994;12:14-43.

LIST OF TABLES

Table 1. Physical properties of graphite powders

Table 2. XRF results with composition indicated as wt.%

Table 3. Cone calorimeter data summary

LIST OF FIGURES

Figure 1. SEM micrographs of and graphite samples: (A) Natural Zimbabwean graphite; (B) Expandable graphite ES250 B5; (C) Exfoliated graphite (low resolution), (D) Exfoliated graphite (high resolution).

Figure 2. TGA traces in air for the expandable graphite, the plasticized PVC and a compound containing 20 wt.% expandable graphite. Temperature was scanned from 25 °C to 900 °C at a scan rate of 10 °C min⁻¹ with air flowing at a rate of 50 mL min⁻¹.

Figure 3. Thermomechanical characterization of the exfoliation process of the expandable graphite. The temperature was scanned at a rate of 10 °C min⁻¹ in nitrogen atmosphere. A flat-tipped standard expansion probe was used and the applied force was 0.02 N.

Figure 4. Cone calorimeter heat release rate curves for the plasticized PVC compound and its composites with expandable graphite. The sample sheets were backed by aluminium foil and their dimensions were 100 mm × 100 mm × 4 mm. They were exposed horizontally to an external heat flux of 35 kW m⁻².

Figure 5. Cone calorimeter peak heat release rates and total heat release for the plasticized PVC compound and its composites with expandable graphite. The sample sheets were backed by aluminium foil and their dimensions were 100 mm × 100 mm × 4 mm. They were exposed horizontally to an external heat flux of 35 kW m⁻².

Figure 6. Cone calorimeter mass loss curves for the plasticized PVC compound and its composites with expandable graphite. The sample sheets were backed by aluminium foil and their dimensions were 100 mm × 100 mm × 4 mm. They were exposed horizontally to an external heat flux of 35 kW m⁻².

Figure 7. Cone calorimeter time to ignition and flame out for the plasticized PVC compound and its composites with expandable graphite.

Figure 8. Cone calorimeter smoke production curves for the plasticized PVC compound and its composites with expandable graphite.

Figure 9. Cone calorimeter CO₂ production curves for the plasticized PVC compound and its composites with expandable graphite.

Figure 10. Cone calorimeter CO production curves for the plasticized PVC compound and its composites with expandable graphite.

Figure 11. Petrella plot for PVC and its expandable graphite composites. Cone calorimeter data were obtained using an external heat flux of 35 kW m⁻² on sheets measuring 100 mm × 100 mm × 4 mm and backed by aluminium foil.

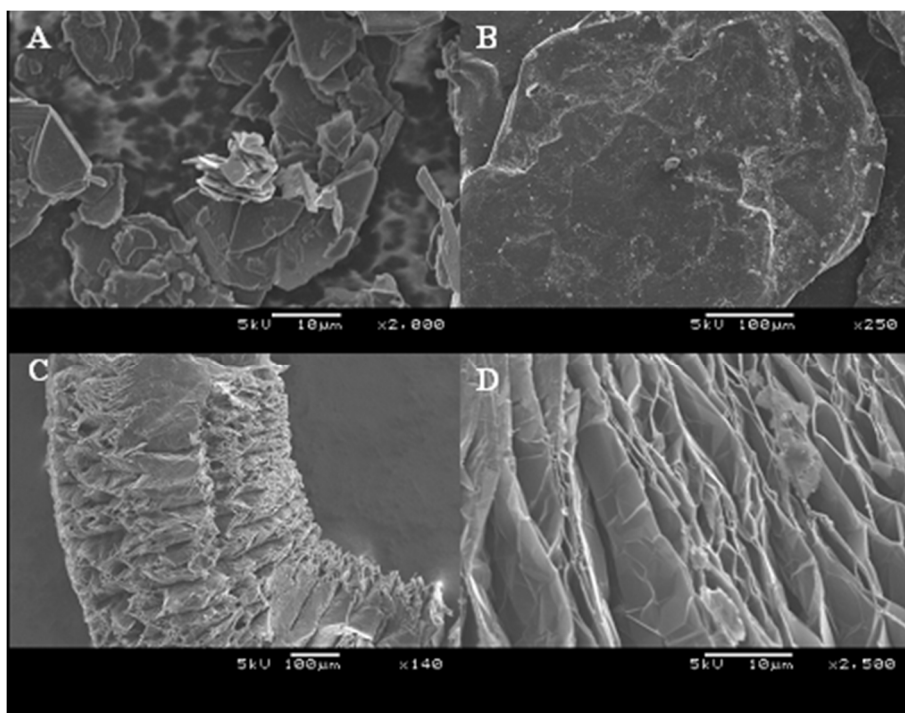


Figure 1. SEM micrographs of and graphite samples: (A) Natural Zimbabwean graphite; (B) Expandable graphite ES250 B5; (C) Exfoliated graphite (low resolution), (D) Exfoliated graphite (high resolution).

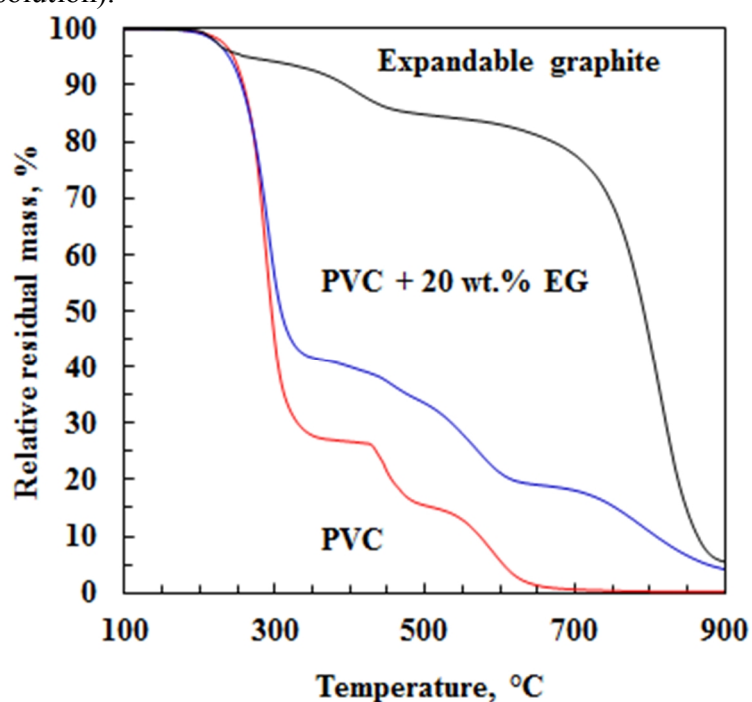


Figure 2. TGA traces in air for the expandable graphite, the plasticized PVC and a compound containing 20 wt.% expandable graphite. Temperature was scanned from 25 °C to 900 °C at a scan rate of 10 °C min⁻¹ with air flowing at a rate of 50 mL min⁻¹.

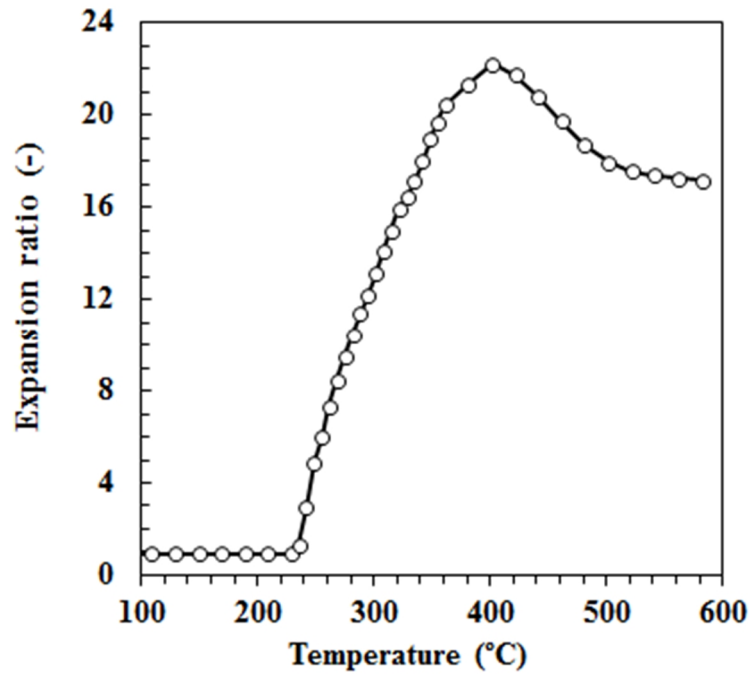


Figure 3. Thermomechanical characterization of the exfoliation process of the expandable graphite. The temperature was scanned at a rate of $10\text{ }^{\circ}\text{C min}^{-1}$ in nitrogen atmosphere. A flat-tipped standard expansion probe was used and the applied force was 0.02 N.

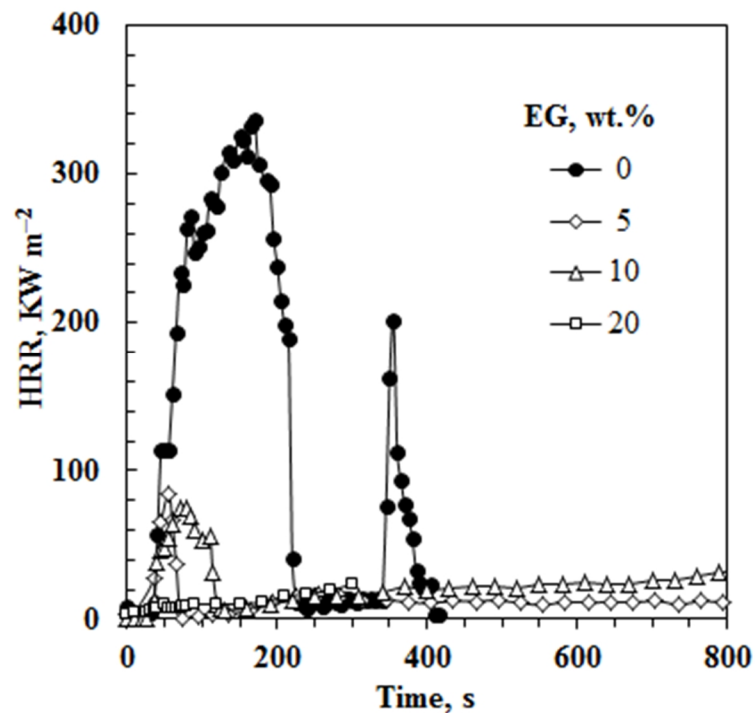


Figure 4. Cone calorimeter heat release rate curves for the plasticized PVC compound and its composites with expandable graphite. The sample sheets were backed by aluminium foil and their dimensions were $100\text{ mm} \times 100\text{ mm} \times 4\text{ mm}$. They were exposed horizontally to an external heat flux of 35 kW m^{-2} .

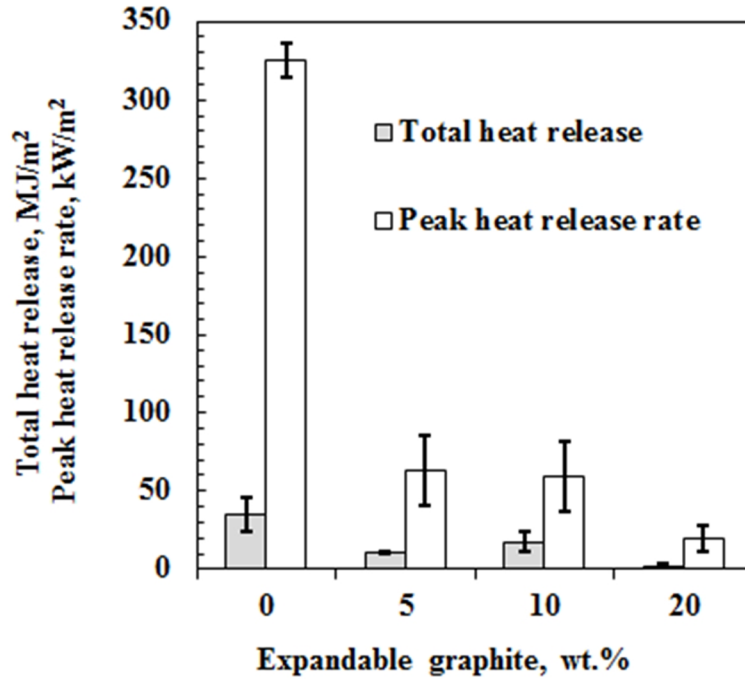


Figure 5. Cone calorimeter peak heat release rates and total heat release for the plasticized PVC compound and its composites with expandable graphite. The sample sheets were backed by aluminium foil and their dimensions were 100 mm × 100 mm × 4 mm. They were exposed horizontally to an external heat flux of 35 kW m⁻².

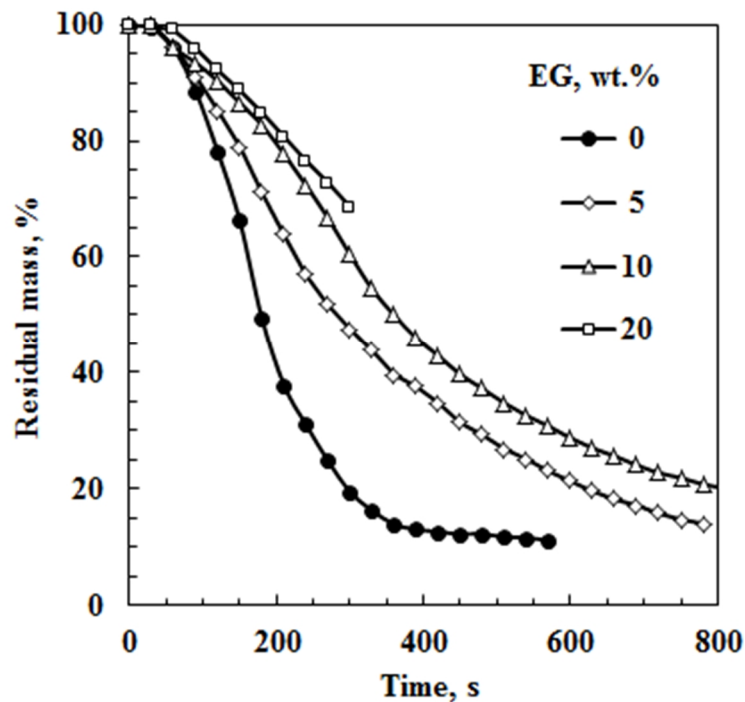


Figure 6. Cone calorimeter mass loss curves for the plasticized PVC compound and its composites with expandable graphite. The sample sheets were backed by aluminium foil and their dimensions were 100 mm × 100 mm × 4 mm. They were exposed horizontally to an external heat flux of 35 kW m⁻².

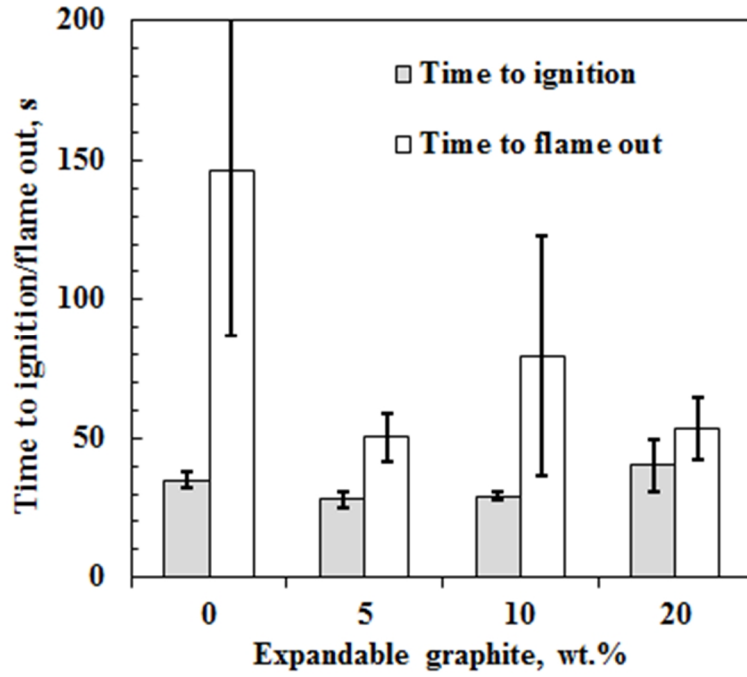


Figure 7. Cone calorimeter time to ignition and flame out for the plasticized PVC compound and its composites with expandable graphite.

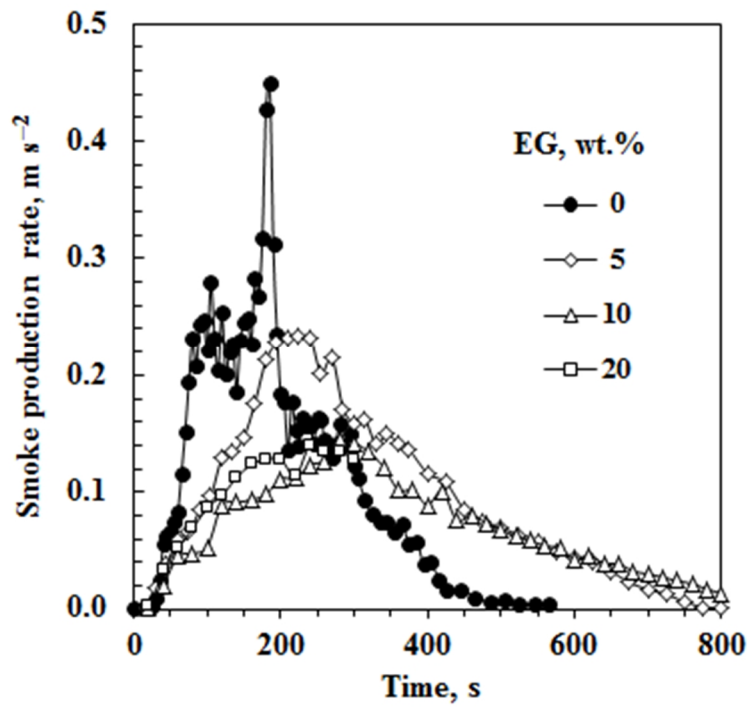


Figure 8. Cone calorimeter smoke production curves for the plasticized PVC compound and its composites with expandable graphite.

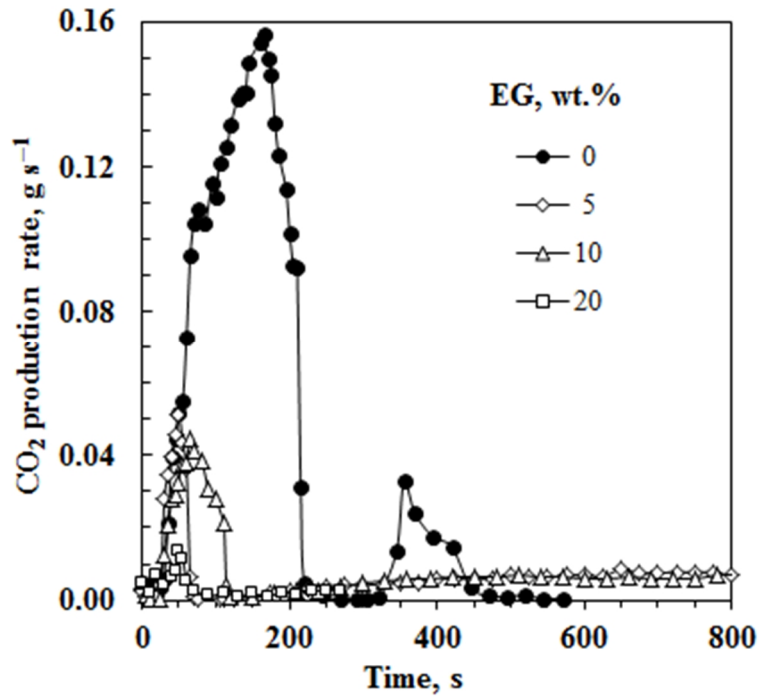


Figure 9. Cone calorimeter CO₂ production curves for the plasticized PVC compound and its composites with expandable graphite.

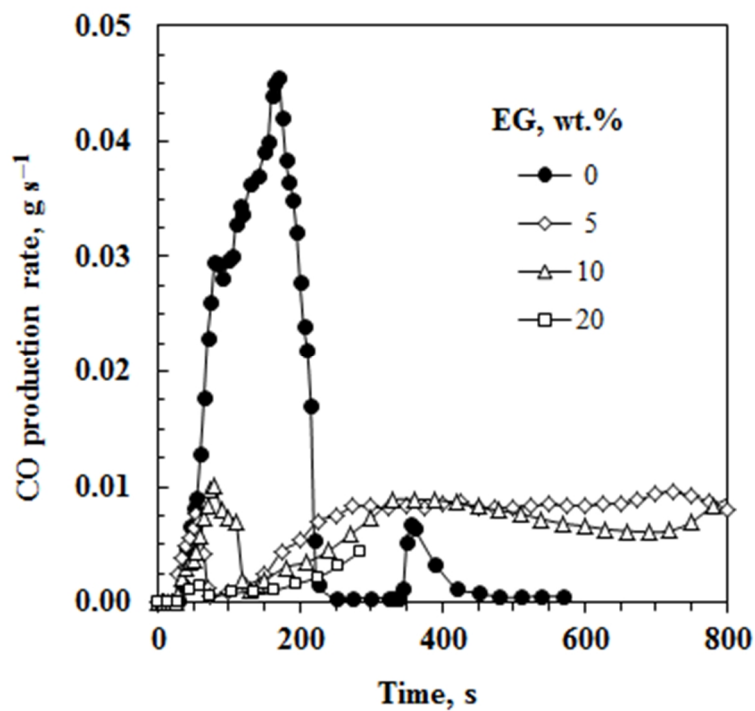


Figure 10. Cone calorimeter CO production curves for the plasticized PVC compound and its composites with expandable graphite.

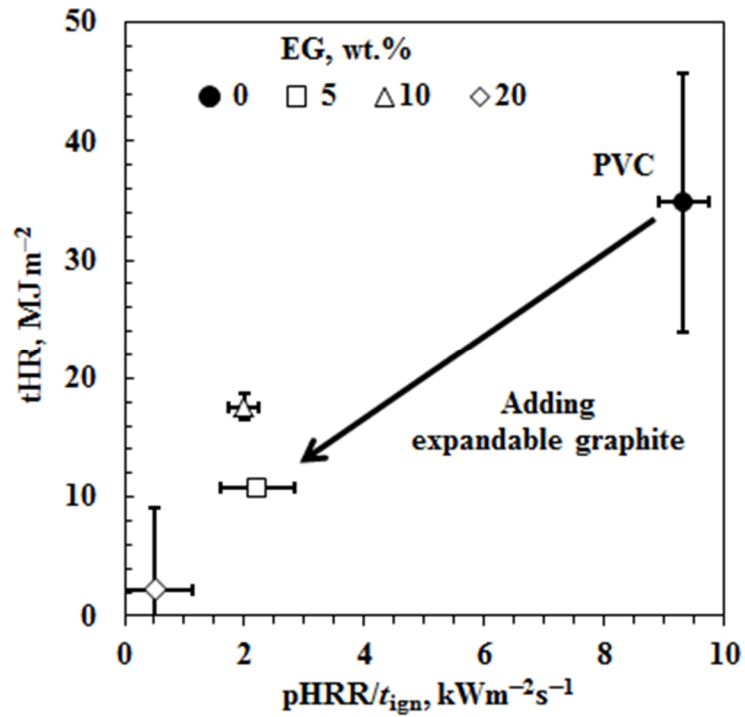


Figure 11. Petrella plot for PVC and its expandable graphite composites. Cone calorimeter data were obtained using an external heat flux of 35 kW m^{-2} on sheets measuring $100 \text{ mm} \times 100 \text{ mm} \times 4 \text{ mm}$ and backed by aluminium foil.